International Journal of Scientific Research in Engineering and Management (IJSREM)
Volume: 07 Issue: 12 | December - 2023 SJIF Rating: 8.176 ISSN: 2582-3930

Solar Powered Marine Water Pumping Fuzzy Logic Controlled Modular Multilevel Inverter

Samiksha patel
Mtech Scholar
Department of Electrical Engineering,
SSTC, Bhilai
samikshapatel97@gmail.com

Tanu Rizvi
Assistant Professor,
Department of Electrical Engineering,
SSTC, Bhilai

Devanand Bhonsle
Sr. Assistant Professor,
Department of Electrical Engineering,
SSTC, Bhilai

Abstract: For maritime water pumping applications, this article details the design and construction of a Modular Multilevel Inverter (MMI) to manage the Induction Motor (IM) drive with smart approaches. The suggested eleven-level inverter can regulate the output of a solar photovoltaic system powering an IM drive. Nearly half of a ship's overall energy consumption is thought to go towards pumping systems. In light of this, this study explores and verifies the suggested low-complexity control architecture for a maritime water pumping system using an induction motor (IM) drive and a magnetic field inductor (MMI). For the purpose of performance enhancement, a Proportional-Integral (PI) controller and a Fuzzy Logic (FL) controller are analyzed and compared for use with the inverter. Better robustness has been compared with regard to peak overshoot, controller settling time, and inverter Total Harmonic Distortion (THD). Designing and integrating MMI, IM drive, and intelligent controller specifically for maritime water pumping applications is the innovation of the proposed control method..

Keywords: Field programmable gate array, fuzzy logic controller, induction motor drive, modular multilevel inverter, proportional- integral, total harmonic distortion.

I. Introduction

The global marine and shipping sectors have made significant contributions to increasing air emissions and energy consumption. International Convention for the Prevention of Pollution from Ships organisation (MARPOL) [1, 2] has established standards that must be adhered to in order to prevent pollution in the maritime environment from both intentional and unintentional sources. About three percent of the world's carbon dioxide emissions come from the diesel engines used in the maritime industry, contributing to climate change and global greenhouse gas emissions [3]. The maritime shipping industry is responsible for 2.8% of global greenhouse gas emissions from diesel engines, 15% of nitrogen oxides, and 13% of sulphur oxides.

Rules and regulations for cutting down on carbon dioxide (CO2) emissions from ships have been exhaustively researched and drafted by the United Nations Framework Convention on Climate Change (UNFCCC) and the International Maritime Organisation (IMO). Depletion of traditional energy sources is causing a rising global energy crisis, and this process also contributes significantly to the release of toxic air and water contaminants. There will be an 8% rise in greenhouse gas and CO2 emissions from the use of diesel engines in ships by 2020 [3, 4]. The shipbuilding sector has always had pollution concerns, but recently there has been a trend towards using solar power to supply clean electricity from green energy sources. With a growing population comes a greater need for electricity, but alternatives like solar power and better inverter technology are emerging as viable solutions [3, 4]. The global energy issue is becoming worse because traditional energy sources are running out. However, it also causes the greenhouse effect, which in turn warms the planet. By the end of this century, scientists predict a 3 to 6 degree Celsius rise in global surface temperatures [4, 5]. Solar power is preferable to other energy sources for most suburban and maritime applications since it is low-maintenance, runs quietly because it has no moving components, and takes up less room on the ship's roof. In order to provide the necessary electricity while simultaneously reducing emissions, increasing renewable energy efficiency, and bolstering power stability, a solar photovoltaics-based energy system is introduced in the ship. In order to connect a wide variety of high-power loads, a solar energy source is combined with a power electronic converter and inverter [6]. The integration of renewable energy sources into power converters has recently been the focus of much research on board contemporary ships. Voltage drift and frequency variations, both of which cause harmonics distortions [7], [8], are two of the most serious problems that can arise in a power converter. The ship's pumping systems use up about 70% of the ship's total electrical energy [9], [10]. Power electronics aboard ships rely heavily on converters for the propulsion of motor drives systems, but this critical component is particularly vulnerable to the negative effects of harmonics. The suggested research delves into the latest innovations of modular inverter, which are employed to enhance power quality on board by decreasing harmonics with the help of an intelligent controller. In this study, we provide a unique symmetric multilevel module built on the cascade category that can generate negative voltage levels without any supplementary circuitry. Figure 1 depicts a solar-powered eleven-level inverter with smart control approaches designed to boost performance in maritime settings. The ship's seawater cooling pump's variable frequency motor is powered by the inverter. With PI and FLC based controllers, we analyse the IM drive's performance when supplied by a multilayer inverter. Most applications requiring speed regulation make use of the proportional-integral (PI) controller due to its superior maximum peak overshoot and stability. The FLC is the simplest intelligent controller available for controlling the speed of induction motors. From daylight to night, the ship's water supply is pumped constantly. An induction motor's starting current and fixed voltage must be properly maintained by inverter management.

The commutation in conventional DC motors is problematic. Induction motors are used on ships because they avoid the problems associated with DC motors. The fresh water is cooled to the ideal temperature because of the saltwater pumps. The proposed study focuses on MMI topology in sustained control approaches for a single-phase IM drive for marine water pumping. Maximum solar power extraction in the atmospheric circumstances governs the real-time execution of speed control. In addition, an inverter's primary function is to regulate the rpm of an induction motor by gradually changing the frequency at which it switches. This is accomplished using a FL controller's optimised Pulse Width Modulation (PWM), which is the result of a modulating signal. The simulation research plans to improve the system's overall performance by planning the building of a solar PV fed MMI that powers an IM drive with PI and FL based controllers. The SPARTAN3E500 FPGA controller used to construct the prototype model generates the pulses required by the inverter and the converter. As an example of the paper's contributions, consider the following: Comparing the effectiveness of PI and FL-based controllers on an IM drive system for pumping seawater The SPARTAN3E500 FPGA controller was used to implement an MMI-fed IM drive in real time. Increasing power quality through a comparison of FL and PI based controllers' effects on performance. The effectiveness of MMI is the primary research topic of this work. The paper is structured as follows: The configuration and operation strategy of the system are presented in Section II, the control technique for the suggested topology is described in Section III, the simulation results are analyzed in Section IV, and the experimental setup and comments are presented in Section V.

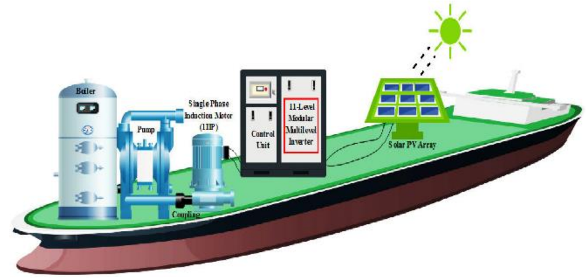

Figure 1: Fuzzy Logic Control for Solar PV Fed Modular

II. LITERATURE REVIEW

D. C. Yu, Y.-Y. Hong, J. Dai, and P. Cheng; H. Lan, Y. Bai, S. Wen; 'The introduction of solar production into ship power systems has gained more attention in recent years due to the growing concern about severe environmental contamination and the usage of fossil energy. Uncertainties in sun irradiation, however, will lead the ship's power system to become unstable as solar energy becomes more widely employed. Photovoltaic (PV) modules aboard ships produce different amounts of energy while the ship rolls than they would on land. In this study, we simulate a big oil tanker with a PV generating system, a diesel generator, a FESS, and several types of ship loads in order to smooth the PV power fluctuations and enhance the power quality. In addition, a constant torque angle control method is provided to regulate the FESS charging and discharging, which is then coupled with a sinusoidal pulse width modulation (SPWM) strategy. The effects of ship rolling and various operational scenarios are considered. The simulation findings show that the flywheel energy storage system improves the stability of the proposed hybrid ship power system due to its high efficiency and rapid reaction.

J. M. Guerrero, Z. Jin, L. Meegahapola, N. Fernando, and S. G. Jayasinghe The widespread use of power electronic interfaced loads and sources has contributed to the current surge in interest in ship microgrids. Aside from the addition of extremely dynamic big loads, such propulsion loads, these microgrids are quite similar to their terrestrial counterparts. Problems with power quality are exacerbated in ship micro grids by the presence of loads and sources equipped with power-electronic converter interfaces. These problems, also known as harmonic distortions, typically manifest themselves as voltage fluctuations, frequency shifts, and waveform distortions. The most promising technique for reducing voltage and/or frequency fluctuations is energy storage, which is one of the recognized options. Most technologies for lowering harmonic distortions rely on passive filtering, which makes use of cumbersome components like capacitors and inductors. An developing option is active filtering, which may be implemented inside the same interface converter as the energy storage device. This study aims to critically analyses power quality challenges, energy storage technologies, and potential solutions for improving power quality in ship microgrids, with an emphasis on current advancements in these areas. Additionally, the study provides a primer on the various ship power system topologies.

According to R. Kumar and B. Singh, a dc-dc conversion step is often required in solar PV fed water pumping that is powered by a brushless dc (BLDC) motor in order to optimize the solar photovoltaic (PV) generated power using a maximum power point tracking approach. There is a negative impact on efficiency, cost, size, and complexity due to the need for a power conversion step. This study discusses a novel approach to this problem—a solar PV energy conversion system that feeds a BLDC motor-pump without the need for a dc-dc converter. For BLDC motors, we present a straightforward control strategy that allows for peak power operation of the solar PV array from a single inverter. The phase current sensors in BLDC motors are unnecessary with the suggested control. The motor-pump's speed and soft start are both independently controlled. Solar PV array optimal power regulates the speed. Performance evaluation utilizing simulated results generated in MATLAB/Simulink and experimental validation on a constructed prototype, under realistic operating circumstances, demonstrate the viability of the proposed system.

Authors: S. Shukla & B. Singh This study discusses a solar-powered, single-stage, vector-controlled, induction motor drive for a water pumping system that eliminates the need for a speed sensor. The stator flux is approximated to provide an approximation of the speed. The suggested setup consists of a motor-pump unit, a three-phase voltage source converter, and a solar photovoltaic (PV) array. To get the most out of a PV array, a maximum power point tracking technique based on incremental conductance is applied. Induction motors benefit from vector control, which allows for a soft start. An experimental prototype is constructed in the lab, and the desired configuration is designed and simulated on the MATLAB/Simulink platform before being verified.

The marine industry is beginning to recognize that variable-frequency-drive (VFD) applications are one of the most successful instruments for energy savings (C.-L. Su, W.-L. Chung, and K.-T. Yu). Since the ambient seawater temperature fluctuates substantially while ships sail between different sea locations, significant energy advantage may be realized with VFD-driven central saltwater cooling systems. The real energy and cost reductions from each drive option must be known before a final selection can be made. In order to accurately predict the economics of its implementation, it is crucial to have access to a quick and easy technique for calculating the energy savings. The purpose of this work is to provide a quick approach for estimating the potential energy savings from retrofitting ships' seawater cooling pumps with variable frequency drives (VFDs). Marine hardware, pipe allocation, ambient seawater temperature, and other navigational and environmental factors like these are considered. In order to correctly use the pump hydraulic formulae, it is necessary to mathematically describe the process system, which includes mechanical, instrumental, and pump hydraulics, as well as the electrical components of the drive. An actual ship's saltwater cooling system's energy-savings evaluations verified the efficacy of the suggested solution. Energy savings and their relation to shipping routes were analyzed in detail. In order to verify the financial viability of variable-speed flow control for comparable systems in industrial settings, the analytical model proposed in this study may be used as a helpful tool.

III. Proposed

Taking into account the rating of the IM drive coupled water pump, a PV array with a maximum power capacity of 150W at Standard Test Conditions (STC) (1000W/m2, 25C) is proposed. With the help of a modular multilevel inverter [11], [12], the working power capacity of the PV array is chosen to power the motor pump system. DESIGN OF PV Arrays There are 36 cells in a 10W solar PV module (36 x 0.588 V = 21.6 Voc). The maximum power is 10Wp, the operating voltage is 21.6V, and the short-circuit current is 0.659 A. A module's maximum voltage (Vmp) is 17V, and its maximum current (Imp) is 0.588A (Pmax = Vmp Imp = 17 0.588= 9.96W). As the power source, we employ a 20W solar module consisting of 72 connected cells in series. The maximum power is 20Wp, the operating voltage is 21.5V, and the short-circuit current is 1.24 A. At Vmp = 17.5V and Imp =1.143A, a module's maximum power output (Pmax = Vmp Imp = 17 1.14 = 19.38W) is reached. The maximum power output of 150 W is achieved by connecting the two separate ratings of 10W and 20W mentioned above in series and parallel (5 10 = 50W, 5 20 = 100W, STC). Attaining the V-I characteristics of the PV cell necessitates satisfying four indefinite restrictions (IL, I0, Rs, and) supplied by the current equation of solar cell presented in equation (1) [13], [14].

$$I = I_L - I_D = I_L - I_0 e^{\left(\frac{V+IR_s}{a}\right)} - 1 \qquad (1)$$

1) ESTIMATION OF LIGHT CURRENT (IL)

A scheme to estimate the light current IL is expressed as,

IL = ϕ ϕref [IL,ref + μI,SC(TC − TC,ref)] (2)

2) ESTIMATION OF SATURATION CURRENT (I0) The expression for saturation current is expressed as,

$$I_0 = I_{0,ref}\left(\frac{T_{C,ref}+273}{T_C+273}\right)^{3}\exp\left[\frac{e_{gapNs}}{q\alpha_{ref}}\left(1-\frac{T_{C,ref}+273}{T_C+273}\right)\right] \quad (3)$$

During the reference condition the saturation current can be evaluated as,

$$I_{0,ref} = I_{L,ref}\exp\left(-\frac{V_{oc,ref}}{\alpha_{ref}}\right) \quad (4)$$

DETERMINATION OF TVTC FACTOR

The Thermal Voltage Timing Completion (TVTC) factor (α) is the task of temperature and expressed as,

$$\alpha_{ref} = \frac{2V_{mp,ref} - V_{oc,ref}}{\frac{I_{sc,ref}}{I_{SC,ref}-I_{mp,ref}} + \ln\left(1-\frac{I_{mp,ref}}{I_{SC,ref}}\right)} \quad (5)$$

$$\alpha = \frac{T_C + 273}{T_{C,ref}+273}\alpha_{ref} \quad (6)$$

DETERMINATION OF SERIES RESISTANCE (Rs)

The series resistance is determined as,

$$R_s = \frac{\alpha_{ref}\ln\left(1-\frac{I_{mp,ref}}{I_{SC,ref}}\right) + V_{OC,ref} - V_{mp,ref}}{I_{mp,ref}} \quad (7)$$

B. DC-DC CONVERTER DESIGN

The solar photovoltaic conversion system utilises an intermediate DC-DC converter that is specifically designed to run at its highest power level in order to provide symmetric input to the MMI. Equation (8) demonstrates the correlation between the input voltage and output voltage of a DC-DC boost up converter in relation to the duty cycle[44].

$$V_{out} = \frac{V_{in}}{1-D} \quad (8)$$

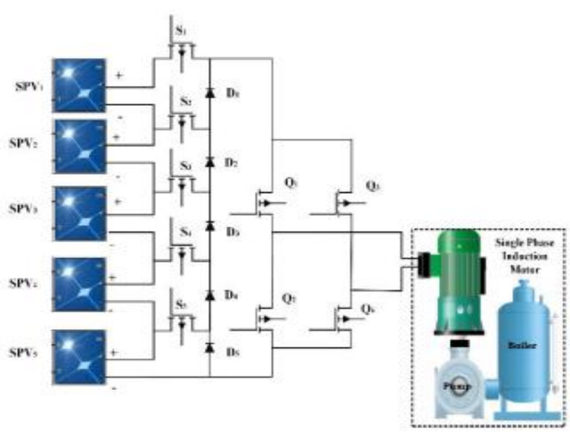

FIGURE 2. Proposed multilevel inverter

1) DESIGN OF AN INDUCTOR (L)

The subsequent procedures outlined by Equations (9)-(10) demonstrate the process of designing an Inductor necessary for the system.

$$L_1 = \frac{V_{in} * (V_{out} - V_{in})}{\Delta I_L * f_s * V_{out}} \quad (9)$$

$$\Delta I_L = (2\% - 4\%) * I_{out(max)} * \frac{V_{out}}{V_{in}} \quad (10)$$

$$\Delta I_L = (0.03) * 5 * \frac{24}{12} = 0.3$$

$$L_{b1} = \frac{12 * (24 - 12)}{0.3 * 3 \times 10^3 * 24} = 0.65$$

C. DESIGN OF A CAPACITOR

The following steps given from Equations (11)-(12) illustrate the design of a Capacitor required for the system.

$$C_1 = \frac{I_{(out)} * D}{f_s * \Delta V_{out}} \quad (11)$$

$$\Delta V_L = (2\% - 4\%) * V_{out(max)} * \frac{I_{out}}{I_{in}} \quad (12)$$

$$\Delta V_L = (0.03) * 24 * \frac{5}{10} = 0.36$$

$$D = \frac{V_{out}}{V_{in} + V_{out}} = \frac{12}{36} = 0.67$$

Vout(max) is the maximum voltage delivered by the PV module under STC.

D. MULTILEVEL INVERTER DESIGN

The voltage separator at the input end consists of a series connection of five solar PV modules labelled as SPV1, SPV2, SPV3, SPV4, and SPV5, as seen in Figure 2[20]. The input voltage is subsequently sent along a pathway consisting of semiconductor devices, including both controlled and uncontrolled components, labelled as S1, S2, S3, S4, S5, D1, D2, D3, D4, and D5. Finally, the voltage reaches an H-bridge, which is composed of Q1, Q2, Q3, and Q4. Equations (13) and (14) demonstrate that the symmetrical modular multilevel structure greatly enhances the quantity of output voltage levels [15].

$$N_{level} = 2S + 1 \quad (13)$$

$$N_{IGBT} = S + 4 \quad (14)$$

1) WATER PUMP DESIGN

The water pumping system consists of an induction motor (IM) drive and a centrifugal pump specifically designed for maritime purposes. The pump affinity rule serves as a benchmark for the design of centrifugal pumps. As stated in equation (15), the load torque is exactly proportional to the square of the speed[26].

$$T_L = K_p \times \omega_r^2$$

$$K_p = \frac{9.94}{(2 \times \pi \times 24)^2} = 0.00043712\text{Nm}/(\text{rad}/\text{sec})^2 \quad (15)$$

IV. CONTROL TOPOLOGY FOR MMI

Figure 3 illustrates the configuration of the marine water pumping system, which utilises a solar PV fueled IM drive and incorporates an MMI. The suggested configuration involves utilising PI and FL based controllers to regulate the MMI. The operation of a multilayer inverter and the speed management of an induction motor are achieved via the use of intelligent control techniques in conjunction with Pulse Width Modulation (PWM). The v/f control system is utilised by adjusting the voltage and frequency, together with the reference, in the Alternate Phase Opposition Disposition (APOD) category of multicarrier PWM schemes. The five distinct triangular carrier waveforms, each with a phase difference of 180 degrees, are compared to a single sinusoidal reference waveform in order to create the necessary PWM pulses, as seen in Figure 4. Both controllers utilise logic control and rule-based approaches to generate a modulating signal. This signal is then compared with the carrier to provide the necessary dynamic pulses for the inverter switches [16], [17]. An analysis is conducted on the performance of IM (Induction Motor) with PI (Proportional-Integral) and Fuzzy controllers under constant and variable loads in both open loop and closed loop operation. The subsequent sections delineate the design and execution of PI and FL controllers in enhancing the efficiency of an Induction Motor (IM) drive working in conjunction with a Motor Mechanical Interface (MMI)..

A. PI CONTROLLER BASED SPEED CONTROL

The PI controller is commonly built using one of three ways: trial and error, evolutionary processes, or specific tuning methods such as Cohen Coon, Lambda tuning, and Ziegler Nichols. When comparing several approaches for tuning a PI controller, the trial and error method is preferred since it has significant advantages in identifying the gain parameters and achieving improved performance in motor driving applications. The comparator typically compares the actual speed (ωrm) and the reference speed (ωrm∗). The resulting error (ωe(n)) is then utilised to adjust the parameters Kp and Ki. The error equation (ωe(n)) is expressed as follows:

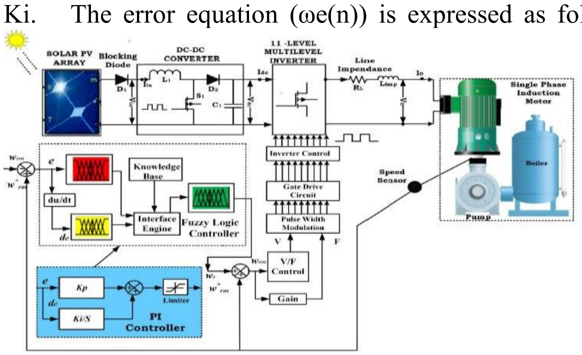

FIGURE 3. Control approach of the proposed inverter.

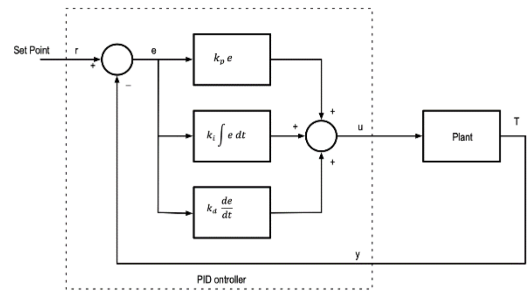

FIGURE 4. Pwm Output Of Pi.

B. FUZZY LOGIC CONTROLLER

Because of its ability to quickly analyse the speed controller while also adding human thought and rule-based procedures, the fuzzy logic controller has become a popular tool for improving electrical equipment. Induction motors can be controlled using one of three primary approaches: (1) the voltage/frequency technique, (2) the flux control method, or (3) the vector control method. Closed loop v/f control is deemed superior than open loop methods of speed regulation because of its ease of use and precision[30].

First, the suggested FL controller has to estimate the speed of an induction motor, and second, it needs to reduce the speed inaccuracy using the rules-based approach without degrading the harmonics.

There are two inputs and one output on the FL controller. The modulating signal is viewed as the output, while the error and its rate of change are used as input. The four major processes of a FL controller are as follows: (1) Input is transformed into fuzzy variables via an analogue fuzzifier (1) Maintains a database of fuzzy rules (2) Inference and related rules

Fourth, the defuzzifier can transform the fuzzy variables into the true goal.

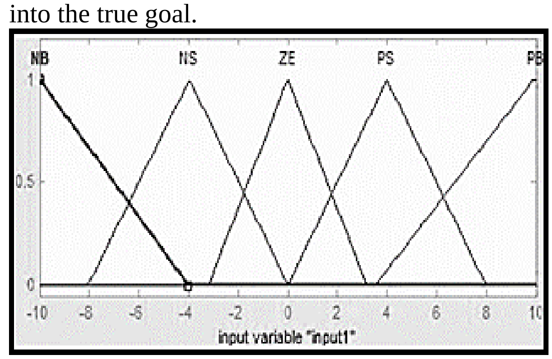

FIGURE 5. Allocation of range for subsets.

TABLE 1. Fuzzy rules.

e/ce		NB	NS	ZE	PS	PB
NB		ZE	NS	NB	NB	NB
NS		ZE	NS	NB	NS	NB
ZE		PB	PS	ZE	NS	NB
PS		PB	PS	PS	ZE	NS
PB		PB	PB	PB	PS	ZE

If the fuzzifier's input variables have two or more relationship values, then those values will be passed on to the fuzzy operator. One truth value is returned as the result. If the error is to be indicated by input 1, then that is what it signifies, whereas input 2 shows whether or not the error is changing. There are eight fuzzy subsets in the linguistic variables, of which five are actually employed.
There are five possible speeds: (1) very slow (very NB), (2) very fast (very NS), (3) very fast (very PS), (4) very fast (very PB), and (5) very slow (very ZE).
Assuming NS as the result, it can take on values up to 0.3416, making it compatible with all rule-based membership functions. Figure 5 depicts the 0.1-volt NB output, 1-volt PB output, 0.66-volt PS output, and 0.5-volt ZE output. There is a wide variety of linguistic input values, including: NB 1600, 10, 4, NS 8.06, 3.96, 0.02646, ZE 3.2, 0, 3.2, PS 0–4, 8–8, and PB 3.52–9.92,1550. The speed-regulating logic, represented as a rule matrix in Table 1, is described below.
Nine semiconductor switches (S1-S5) are paralleled with four H bridge switches (Q1-Q4) to form the 11-level MMI. Fuzzy rules are used to compare bipolar triangular and sine waves to create the PWM. Inverter control pulses are denoted by S1 through S5, whereas level control pulses are denoted by Q1 through Q4.

Figure 6 depicts the whole design process for an FLC, which is driven by the switching pattern of the inverter and the switching pulse generator. Membership in the input fuzzification is planned (IN1-IN6)[35].

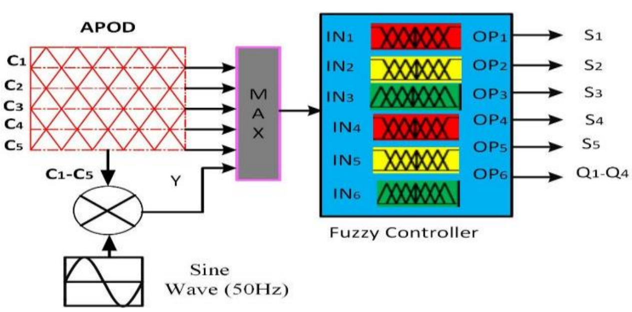

FIGURE 6. FLC controller switching pulse generation structure.

with switching magnitude range of (1, 0, 1). Positive range from 0 to 1 represents the first quarter cycle (0°-90°) and second quarter cycle (90°-180°) respectively. Similarly, the negative range from 1 to 0 represents the third quarter cycle (180°-270°) and fourth quarter cycle (270°-360°). Later,in defuzzification, six membership functions are developed based on fuzzy rules to obtain the desired output.

The paper illustrates the design and development of two controllers for water pumping application. The voltage and frequency are used to control the inverter. The speed of induction motor is controlled by v/f method.

V. SIMULATION AND ITS ANALYSIS

The simulation model is developed in MATLAB/Simulink 2013 to perform the performance comparison between PI and FL based controllers. The analysis for harmonics reduction under open and closed loop operation is also undertaken.

A. SPEED TRACKING PERFORMANCE AND HARMONICS ANALYSIS OF INVERTER

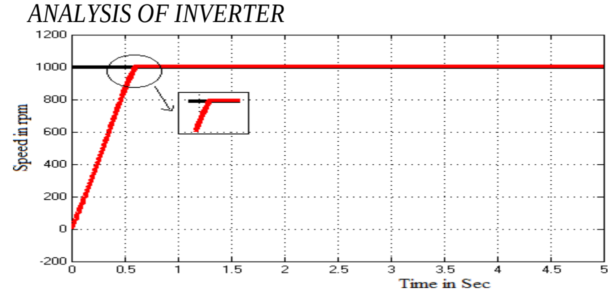

The intended speed range for the IM drive linked to the pump is 0 to 1000 rpm. When comparing PI with FLC, it is seen that the parameters of overshoot, undershoot, and steady-state error are larger in PI in order to achieve the required speed. Both controllers are evaluated at the specified reference speed of 1000 revolutions per minute. The FLC-based induction motor drive technology achieves the necessary speed in the shortest possible time.
The simulation result, seen in Figure 7, illustrates the motor commencing at 0 seconds and reaching a stable speed of around 1000 rpm within 2 seconds using a PI controller. The motor initiates at 0 seconds and stabilizes at 0.5 seconds using the FL controller, as seen in Figure 8[39].
The findings are compared based on their optimal gains and faster setup time. The power quality analysis reveals that the Total Harmonic Distortion (THD) is 10.44% when using the PI controller, as depicted in Figure 9. Conversely, while employing the FL controller, the THD is 5.67%, as illustrated in Figure 10. The Field-Oriented Control (FLC) for motor-fed Matrix Converter Modulation Index (MMI) has excellent performance in accurately following speed reference signals and achieving reduced Total Harmonic Distortion (THD). The voltage produced by an 11-level inverter may be shown in Figure 11. The suggested IM

International Journal of Scientific Research in Engineering and Management (IJSREM)
Volume: 07 Issue: 12 | December - 2023 SJIF Rating: 8.176 ISSN: 2582-3930

drive is included into the water pump system specifically designed for maritime applications.

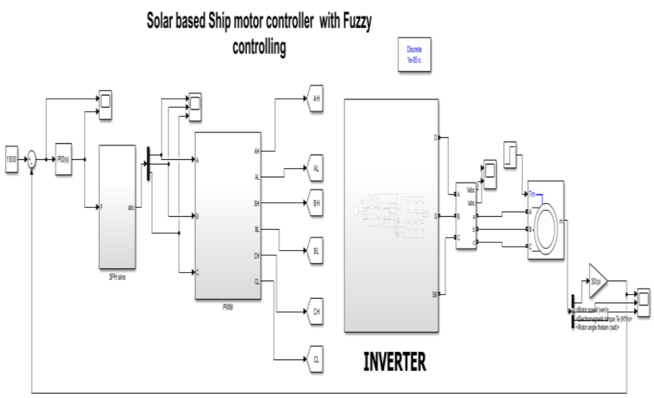

Figure 6(a) Simulink model of Proposed system

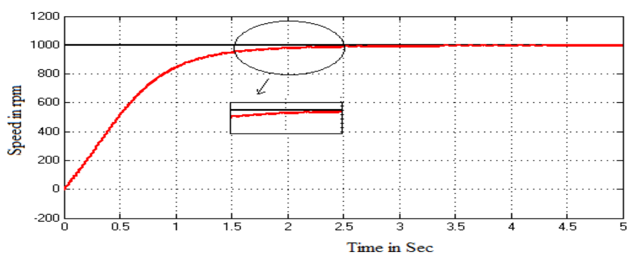

FIGURE 7. Speed response of PI controller at 1000 rpm.

FIGURE 8. Speed response of FLC at 1000 rpm.

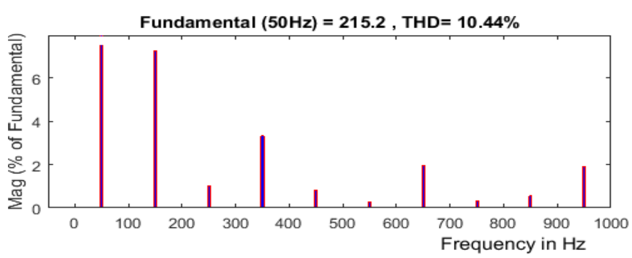

FIGURE 9. Harmonic analysis with PI controller.

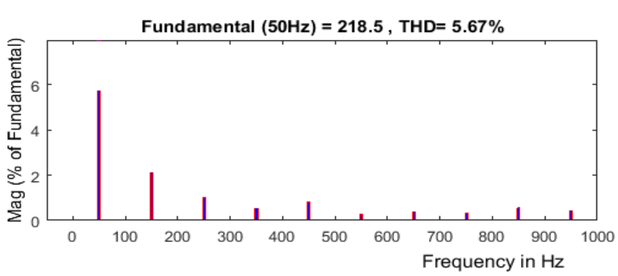

FIGURE 10. Harmonic analysis with FL controller.

VI. CONCLUSION

The significance of the proposed research is to ensure the provision of superior input power to the inverter drive specifically for maritime water pumping applications. An investigation was conducted to assess the feasibility of a solar photovoltaic (PV) fed motor mechanical interface (MMI) for controlling the speed of an induction motor drive. The study focused on examining the steady state and dynamic behaviors of the system, with the aim of determining its compatibility for use in a water pumping system designed for maritime applications. The solar photovoltaic (PV) array is linked to the intended inverter, which then supplies power to an induction motor. The motor speed is detected and the controller receives this information to generate appropriate PWM pulses for the inverter switches. The motor is progressively initiated and the speed is escalated in order to get the desired reference speed, utilizing PI (Proportional-Integral) and FL (Fuzzy Logic) based controllers. The efficacy of PI and FL controllers for a viable operation is validated and the outcomes are compared in both simulation and experimentation. The findings confirm that the FL based controller offers a rapid settling time and less harmonics in comparison to the PI controller. The primary effect of the suggested control strategy is to decrease the steady-state error of the speed control for the induction motor, while simultaneously causing a degradation in the harmonics present in the output voltage of the modular multilevel inverter.

Table 3 provides a comparative comparison of the number of semiconductor switches required for the proposed MMI design and the number of inverters found in existing literature.

The primary constituents of a DC micro grid include the source, converter, load, controller, and grid. A micro grid is typically defined as an independent and self-sufficient system that generates power for a specific town or region. The suggested system includes the whole component required for the DC micro grid, which operates efficiently and fulfils its intended purpose. The future scope is in accurately estimating the generated power and the power used.

REFERENCES

1. Rizvi. T., Dubey. S. P., Tripathi. N. and Makhija. S. P.2022. *FSPV-grid integrated system for efficient electrification of industrial subsection with grid price sensitivity analysis*. IEEE Sponsored Second International Conference on Advances in Electrical, Computing, Communications and Sustainable Technologies (ICAECT 2023).
2. Rizvi. T., Dubey. S. P., Tripathi. N. and Makhija. S. P.2022.*A Comparative Analysis of FSPV-Grid and Grid-*

only systems for an Industrial Subsection. IEEE Sponsored Second International Conference on Advances in Electrical, Computing, Communications and Sustainable Technologies (ICAECT 2022).

3. Rizvi. T., Dubey. S. P., Tripathi. N., Srivastava. S., Makhija. S. P. and Mohiddin. Md. K.2023.*FSPV-Grid system for an Industrial subsection with PV price sensitivity analysis.* Sustainability2023,15(03):1-18.
4. Rizvi. T., Dubey. S. P. and Tripathi. N.2021.*Designing of a Feasible Low Pollutant Grid Integrated System for Steel Plant*. CSVTU Research Journal, 10(02):144-154.
5. Rizvi. T., Tripathi. N.and Dubey. S. P. 2020 *Feasibility Analysis of a Grid Integrated Renewable Energy Systems in Heavy Industries*. Jour of Adv Research in Dynamical & Control Systems (JARDCS),12(06):2289-2302.
6. Rizvi. T., Dubey. S. P. and Tripathi. N.2022.*Reconceptualizing the Application of Renewable Energy Sources in Industry: A Review*. International Research Journal of Engineering and Technology (IRJET), 09(01):514-518.
7. Nirmal. S.and Rizvi. T.2022. *A Review of Renewable Energy Systems for Industrial Applications*. International Journal for Research in Applied Science & Engineering Technology (IJRASET), 10(9): 1740-1745.
8. Nirmal. S., Rizvi. T. and Bhonsle. D.2023. *Design and optimization of grid integrated renewable energy system*. IEEE Sponsored Second International Conference on Advances in Electrical, Computing, Communications and Sustainable Technologies (ICAECT 2023).
9. Chandra. S. and Rizvi. T. 2022. *Detailed Energy Audit of Thermal Power Plant.* International Journal for Research in Applied Science & Engineering Technology (IJRASET), 10(5): 1836-1846.
10. Chandra. S. and Rizvi. T. 2022. *Energy Audit of Thermal Power Plant: A Literature Survey* i-Manager Journal on Power System Engineering, 09(04): 36- 40.
11. Verghese. M. and Rizvi. T. 2023.*Optimal DG Placement for Loss Minimization and Voltage Profile Improvement using Optimization Techniques: A Review*, International Journal of Innovative Research in Engineering (IJIRE),4(2):359-363.
12. H. Lan, Y. Bai, S. Wen, D. C. Yu, Y.-Y. Hong, J. Dai, and P. Cheng, ‘‘Mod- eling and stability analysis of hybrid PV/diesel/ESS in ship power system,’’ *Inventions*, vol. 1, no. 5, pp. 1–16, 2016, doi: 10.3390/inventions1010005.
13. S. G. Jayasinghe, L. Meegahapola, N. Fernando, Z. Jin, and J. M. Guerrero, ‘‘Review of ship microgrids: System architectures, storage technologies and power quality aspects,’’ *Inventions*, vol. 2, no. 4, pp. 1–19, 2017, doi: 10.3390/inventions2010004.
14. R. Kumar and B. Singh, ‘‘Single stage solar PV fed brushless DC motor driven water pump,’’ *IEEE J. Emerg. Sel. Topics Power Electron.*, vol. 5, no. 3, pp. 1337–1385, Sep. 2017, doi: 10.1109/JESTPE.2017.2699918.
15. S. Shukla and B. Singh, ‘‘Single-stage PV array fed speed sensor- less vector control of induction motor drive for water pumping,’’ *IEEE Trans. Ind. Appl.*, vol. 54, no. 4, pp. 3575–3585, Jul./Aug. 2018, doi: 10.1109/TIA.2018.2810263.
16. C.-L. Su, W.-L. Chung, and K.-T. Yu, ‘‘An energy-savings evaluation method for variable-frequency-drive applications on ship central cool- ing systems,’’ *IEEE Trans. Ind. Appl.*, vol. 50, no. 2, pp. 1286–1297, Mar./Apr. 2014, doi: 10.1109/TIA.2013.2271991.
17. B. Singh, U. Sharma, and S. Kumar, ‘‘Standalone photovoltaic water pumping system using induction motor drive with reduced sensors,’’ *IEEE Trans. Ind. Appl.*, vol. 54, no. 4, pp. 3645–3655, Jul./Aug. 2018, doi: 10.1109/TIA.2018.2825285.
18. A. Dolatabadi and B. Mohammadi-Ivatloo, ‘‘Stochastic risk-constrained optimal sizing for hybrid power system of merchant marine vessels,’’ *IEEE Trans. Ind. Informat.*, vol. 14, no. 12, pp. 5509–5517, Dec. 2018, doi: 10.1109/TII.2018.2824811.
19. H.-L. Tsai, ‘‘Design and evaluation of a photovoltaic/thermal-assisted heat pump water heating system,’’ *Energies*, vol. 7, no. 5, pp. 3319–3338, May 2014, doi: 10.3390/en7053319.
20. M. G. Yu, Y. Nam, Y. Yu, and J. Seo, ‘‘Study on the system design of a solar assisted ground heat pump system using dynamic simulation,’’ *Energies*, vol. 9, no. 4, pp. 1–17, 2016, doi: 10.3390/en9040291.
21. S. V. Giannoutsos and S. N. Manias, ‘‘A systematic power-quality assess-ment and harmonic filter design methodology for variable-frequency drive application in marine vessels,’’ *IEEE Trans. Ind. Appl.*, vol. 51, no. 2, pp. 1909–1919, Mar. 2015, doi: 10.1109/TIA.2014.2347453.
22. C. Gnanavel and S. A. Alexander, ‘‘Experimental validation of an eleven level symmetrical inverter using genetic algorithm and queen bee assisted genetic algorithm for solar photovoltaic applications,’’ *J. Cir- cuits, Syst. Comput.*, vol. 27, no. 13, pp. 1–23, 2018, doi: 10.1142/S0218126618502122.
23. R. Thangaraj, T. R. Chelliah, M. Pant, A. Abraham, and C. Grosan, ‘‘Optimal gain tuning of PI speed controller in induction motor drives using particle swarm optimization,’’ *Log. J. IGPL*, vol. 19, no. 2, pp. 343–356, Apr. 2011, doi: 10.1093/jigpal/jzq031.
24. M. S. Zaky and M. K. Metwaly, ‘‘A performance investigation of a four-switch three-phase inverter-fed IM drives at low speeds using fuzzy logic and PI controllers,’’ *IEEE Trans. Power Electron.*, vol. 32, no. 5, pp. 3741–3753, May 2017, doi: 10.1109/TPEL.2016.2583660.
25. R. E. Geneidy, K. Otto, P. Ahtila, P. Kujala, K. Sillanpää, and
26. T. Mäki-Jouppila, ‘‘Increasing energy efficiency in passenger ships by novel energy conservation measures,’’ *J. Mar. Eng. Technol.*, vol. 17, no. 2, pp. 85–98, May 2018, doi:

10.1080/20464177.2017.1317430.

27. A. A. Stonier, ''Design and development of high performance solar photovoltaic inverter with advanced modulation techniques to improve power quality,'' *Int. J. Electron.*, vol. 104, no. 2, pp. 174–189, Feb. 2017.
28. K. Vanchinathan and K. R. Valluvan, ''A Metaheuristic optimization approach for tuning of fractional-order PID controller for speed control of sensorless BLDC motor,'' *J. Circuits, Syst. Comput.*, vol. 27, no. 8, Jul. 2018, Art. no. 1850123.
29. M. Paramasivan, M. M. Paulraj, and S. Balasubramanian, ''Assorted carrier-variable frequency-random PWM scheme for voltage source inverter,'' *IET Power Electron.*, vol. 10, no. 14, pp. 1993–2001, Nov. 2017.
30. E. Babaei, S. Laali, and Z. Bayat, ''A single-phase cascaded multi- level inverter based on a new basic unit with reduced number of power switches,'' *IEEE Trans. Ind. Electron.*, vol. 62, no. 2, pp. 922–929, Feb. 2015, doi: 10.1109/tie.2014.2336601.
31. R. S. Alishah, S. H. Hosseini, E. Babaei, and M. Sabahi, ''Optimal Design of New Cascaded Switch-Ladder Multilevel Inverter Structure,'' *IEEE Trans. Ind. Electron.*, vol. 64, no. 3, pp. 2072–2081, Mar. 2017, doi: 10.1109/TIE.2016.2627019.
32. H. N. Avanaki, R. Barzegarkhoo, E. Zamiri, Y. Yang, and F. Blaabjerg, ''Reduced switch-count structure for symmetric multilevel inverters with a novel switched-DC-source submodule,'' *IET Power Electron.*, vol. 12, no. 2, pp. 311–321, Feb. 2019, doi: 10.1049/iet-pel.2018.5089.
33. E. Samadaei, A. Sheikholeslami, S. A. Gholamian, and J. Adabi, ''A square T-type (ST-type) module for asymmetrical multilevel inverters,'' *IEEE Trans. Power Electron.*, vol. 33, no. 2, pp. 987–997, Feb. 2018, doi: 10.1109/TPEL.2017.2675381.
34. H. Azeem, S. Yellasiri, V. Jammala, B. S. Naik, and A. K. Panda, ''A fuzzy logic based switching methodology for a cascaded H-bridge multilevel inverter,'' *IEEE Trans. Power Electron.*, vol. 34, no. 10, pp. 9360–9364, Oct. 2019, doi: 10.1109/TPEL.2019.2907226.
35. J. Talla, V. Q. Leu, V. Šmídl, and Z. Peroutka, ''Adaptive speed control of induction motor drive with inaccurate model,'' *IEEE Trans. Ind. Electron.*, vol. 65, no. 11, pp. 8532–8542, Nov. 2018.
36. P. R. Bana, K. P. Panda, R. T. Naayagi, P. Siano, and G. Panda, ''Recently developed reduced switch multilevel inverter for renewable energy inte- gration and drives application: Topologies, comprehensive analysis and comparative evaluation,'' *IEEE Access*, vol. 7, pp. 54888–54909, 2019, doi: 10.1109/ACCESS.2019.2913447.
37. P. Omer, J. Kumar, and B. S. Surjan, ''A review on reduced switch count multilevel inverter topologies,'' *IEEE Access*, vol. 8, pp. 22281–22302, 2020, doi: 10.1109/ACCESS.2020.2969551.
38. C. Verdugo, J. I. Candela, and P. Rodriguez, ''Energy balancing with wide range of operation in the isolated multi-modular converter,'' *IEEE Access*, vol. 8, pp. 84479–84489, 2020, doi: 10.1109/ACCESS.2020.2992227.
39. D. Lyu, Y. Sun, C. A. Teixeira, Z. Ji, J. Zhao, and Q. Wang, ''A modular multilevel dual buck inverter with adjustable discontinu- ous modulation,'' *IEEE Access*, vol. 8, pp. 31693–31709, 2020, doi: 10.1109/ACCESS.2020.2972906.\
40. E.-J. Lee, S.-M. Kim, and K.-B. Lee, ''Modified phase-shifted PWM scheme for reliability improvement in cascaded H-bridge multilevel inverters,'' *IEEE Access*, vol. 8, pp. 78130–78139, 2020, doi: 10.1109/ ACCESS.2020.2989694.
41. A. Sabry, Z. M. Mohammed, F. H. Nordin, N. H. N. Ali, and S. Al-Ogaili, ''Single-phase grid-tied transformerless inverter of zero leakage current for PV system,'' *IEEE Access*, vol. 8, pp. 4361–4371, 2020, doi: 10.1109/ACCESS.2019.2963284.
42. A. A. Stonier, S. Murugesan, R. Samikannu, S. K. Venkatachary, S. S. Kumar, and P. Arumugam, ''Power quality improvement in solar fed cascaded multilevel inverter with output voltage regulation tech- niques,'' *IEEE Access*, vol. 8, pp. 178360–178371, 2020, doi: 10.1109/ ACCESS.2020.3027784.